SHUNT REACTIVE POWER COMPENSATION OF LONG TRANSMISSION LINES

Q. Wang, SS Choi
Nanyang Technological University
Singapore 639798
esschoi@ntu.edu.sg

Abstract – The effectiveness of shunt reactive power compensation for long-distance radial transmission is re-examined. Distributed parameter line model is used in the analysis, in which it is shown that the amount of shunt reactive power compensation required is higher if line losses are included. By extending the investigation to include sending-end and receiving-end impedances, generalized expressions on the power transfer limit across the transmission system have been obtained. Steady-state stability limit of the transmission system through mid-point compensation can be readily evaluated using the analytical expressions obtained. Accuracy of the stability analysis is verified through digital simulation studies.

Keywords: transmission line, shunt compensators, maximum power transfer, stability limit.

1   INTRODUCTION

A fundamental requirement in AC power transmission is the maintenance of appropriate network voltage levels. Modern power systems are not very tolerant of abnormal voltages, even for short periods. Whereas active power is generated and absorbed at specific points in the system, reactive power is generated and absorbed in significant quantities throughout the whole system. It also tends to vary with system conditions [1]. In situations where it is difficult to install new transmission circuits, existing facilities are relied on to transfer ever more power. The voltage control problem is exacerbated and the electrical networks are even more stressed. Thus research in AC transmission is centered on how to increase power transfer limit in the most economical manner.

A lossless line operating at its surge impedance loading (SIL) has a flat voltage profile; that is, the voltage magnitude is the same everywhere along the line. No reactive power flow will be observed on the line and the power delivery system is most efficient in term of the delivery of real power. However, as it is not practicable to force the load on a transmission line to coincide with the line SIL at all time, the alternative is to control the SIL so that it matches exactly with the load. Reference [2] describes very well this concept of modifying the surge impedance of a transmission line through rapid shunt compensation control so that the corresponding line SIL equals to the actual loading. Practical shunt compensation scheme would consist of reactive compensators being connected at line ends and at strategic intermediate nodes along the line. Fast-acting shunt compensators such as Static VAr Compensators (SVC) are used to realize the scheme. Voltage support capability

can be exploited and the transmission distance is reduced artificially. As pointed out and theoretically proven in [3, 4], it is well known a mid-point compensated line can transmit up to 2 times the power of the uncompensated line while maintaining steady-state stability. However in a recent article [5], Huang and Ooi presented results of digital simulation studies of such a mid-point compensated transmission system and showed that the ratio is actually close to 1.59. The authors attributed the reduction in term of the distributed capacitance of the line and the finite source-end and receiving-end reactances used in their studies.

In most studies reported in the literature, lossless transmission line models were used. While reference [5] has also attributed the presence of line resistances in contributing toward the reduction in the steady-state stability limit, the authors have not provided any quantitative evidence to support the claim. In the present work, the exact long-line model would be used in the analysis. The purpose is to determine the required shunt compensation to achieve a given power transfer. It is shown that line resistance can affect the accuracy of the line reactive compensation calculation significantly, especially when the transmitted power is above the line natural load and as the line length increases. On the prediction of maximum power transfer (P_{rmax}), although P_{rmax} may be obtained using the approach based on simplified line model [6, 7], generalized expressions with exact representation of the transmission line have yet to be obtained. Such expressions will be included in this paper. The results are obtained by including the sending-end (SE), receiving-end (RE) impedances and the application of mid-point compensation. The accuracy of the analysis is supported through digital simulation studies which show that steady-state stability limit can indeed be predicted more accurately compared to previous works. The analysis provides an improved evaluation of the contribution made by midpoint shunt compensator in enhancing network stability. It quantifies the extent of the improvement in stability through mid-point compensation, as it is affected by such factors as line losses, line length, and SE and RE terminal impedances.

2   ANALYSIS

2.1 Compensation at Line Terminals

As explained earlier, practical compensation scheme would include shunt compensators connected at the terminals of long-lines. The problem thus becomes one of predicting the amount of reactive power needed at

each line terminal so as to maintain the terminal voltage at its nominal value. In previous works [2-7], the authors used various types of approximated line model in their analysis. Of course, physical transmission lines do contain resistances and shunt capacitances. Hence, the so-called exact long-line model which includes line loss would be the starting point of the investigation.
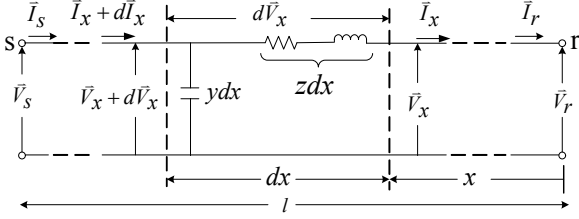
Figure 1: Transmission line model.

The long-line model is as shown in Figure 1, where $\bar{z} = R + j\omega L$ is the series impedance per unit length/phase, and $\bar{y} = G + j\omega C$ is the shunt admittance per unit length/phase of the line. The physical meanings of the various parameters are described in [9]. Line length is l. The focus of the present work is on the behavior of the network at fundamental frequency. Mutual coupling between phases has been ignored.

Let $\bar{Z}_c = \sqrt{\bar{z}/\bar{y}}$, $\bar{\gamma} = \sqrt{\bar{y}\bar{z}} = \alpha + j\beta$. $\bar{Z}_c$ is called the characteristic impedance of the line. $\bar{\gamma}$ is the line propagation constant: α being the line attenuation constant and β the line phase constant. These equations constitute the distributed parameter model of the transmission line. Note that line losses and shunt capacitance have been included. For a lossless line, $\bar{Z}_c$ is commonly referred as the line surge impedance $Z_0 = \sqrt{L/C}$ and has the dimension of a pure resistance. The power delivered by a transmission line when it is terminated by its surge impedance is known as the natural load or SIL denoted as P_0, where $P_0 = V_0^2 / Z_0$, and V_0 is the rated voltage of the line.

Let $\bar{Z}_c = R_c + jX_c$ and the line angle $\theta = \beta l$. Select $\bar{V}_r$ as the reference voltage and denote δ as the phase angle difference by which $\bar{V}_s$ leads $\bar{V}_r$. That is $\bar{V}_r = V_r \angle 0$, $\bar{V}_s = V_s \angle \delta$. Suppose the intention is to make the SE and RE voltage magnitudes equal to V_0. The active and reactive powers at the receiving and sending ends of the line

can be derived and expressed in term of P_0. These are shown as equations (1) - (4), the detailed derivation is presented in Appendix A.

There are now sufficient analytical expressions obtained from which the reactive power requirements at line terminals can be determined. This is because once V_r, V_s, P_r (or P_s) are specified, the power angle δ can be obtained using (1) (or (3)) as line parameters θ and α are known. The required Q_r and Q_s can then be determined using (2) and (4) respectively.

The case of lossless lines becomes a special case of the above when $R = G = 0$. Equations (1)- (4) then degenerate into (5)-(6). These are the familiar results shown in previous works, e.g. in [2, 8].

$$P_r / P_0 = P_s / P_0 = \sin \delta / \sin \theta \qquad (5)$$

$$Q_r / P_0 = -Q_s / P_0 = (\cos \delta - \cos \theta) / \sin \theta \qquad (6)$$

The analytical expressions obtained earlier can also be used to determine the required reactive power for multi-circuit lines. In approaching the ideal practice of having close to a flat voltage profile across the line, the amount of the shunt reactive compensation at each bus is the sum of all the shunt compensation required of each line end connected to the bus. The required shunt compensation at the terminals of each line is of course governed by (1)-(4).

2.2 Midpoint Compensation

Figure 1 provides a complete description of the voltage/current relationship of the transmission lines. However, for purposes of analysis involving interconnection with other network elements, it is more convenient to use equivalent circuits which only describe the characteristics of the lines at their terminals. A π-circuit, as shown in Figure 2 can be used for this purpose [9]. It is also known as the Telegraph model. In term of the line parameters shown in Figure 2, $\bar{Z}_e = \bar{Z}_c \sinh(\bar{\gamma}l)$ and $\bar{Y}_e / 2 = \tanh(\bar{\gamma}l/2)/\bar{Z}_c$.
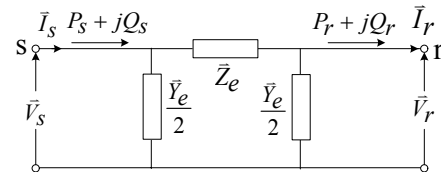
Figure 2: Equivalent π circuit model of a transmission line.

$$P_r / P_0 = \mathrm{Re}\left(\bar{V}_r \bar{I}_r^*\right)\big/P_0 = Z_0 R_c \left[2V_s V_r e^{\alpha l}\cos(\theta-\delta) - 2V_s V_r e^{-\alpha l}\cos(\theta+\delta) + V_r^2(e^{-2\alpha l} - e^{2\alpha l})\right]\big/\left[V_0^2(R_c^2 + X_c^2)(e^{2\alpha l} + e^{-2\alpha l} - 2\cos 2\theta)\right]$$
$$- Z_0 X_c \left[2V_s V_r e^{\alpha l}\sin(\theta-\delta) + 2V_s V_r e^{-\alpha l}\sin(\theta+\delta) - 2V_r^2 \sin 2\theta\right]\big/\left[V_0^2(R_c^2 + X_c^2)(e^{2\alpha l} + e^{-2\alpha l} - 2\cos 2\theta)\right] \qquad (1)$$

$$Q_r / P_0 = \mathrm{Im}\left(\bar{V}_r \bar{I}_r^*\right)\big/P_0 = Z_0 X_c \left[2V_s V_r e^{\alpha l}\cos(\theta-\delta) - 2V_s V_r e^{-\alpha l}\cos(\theta+\delta) + V_r^2(e^{-2\alpha l} - e^{2\alpha l})\right]\big/\left[V_0^2(R_c^2 + X_c^2)(e^{2\alpha l} + e^{-2\alpha l} - 2\cos 2\theta)\right]$$
$$+ Z_0 R_c \left[2V_s V_r e^{\alpha l}\sin(\theta-\delta) + 2V_s V_r e^{-\alpha l}\sin(\theta+\delta) - 2V_r^2 \sin 2\theta\right]\big/\left[V_0^2(R_c^2 + X_c^2)(e^{2\alpha l} + e^{-2\alpha l} - 2\cos 2\theta)\right] \qquad (2)$$

$$P_s / P_0 = \mathrm{Re}\left(\bar{V}_s \bar{I}_s^*\right)\big/P_0 = Z_0 R_c \left[(e^{2\alpha l} - e^{-2\alpha l})V_s^2 - 2V_s V_r e^{\alpha l}\cos(\theta+\delta) + 2V_s V_r e^{-\alpha l}\cos(\theta-\delta)\right]\big/\left[V_0^2(R_c^2 + X_c^2)(e^{2\alpha l} + e^{-2\alpha l} - 2\cos 2\theta)\right]$$
$$- Z_0 X_c \left[2V_s^2 \sin 2\theta - 2V_s V_r e^{\alpha l}\sin(\theta+\delta) - 2V_s V_r e^{-\alpha l}\sin(\theta-\delta)\right]\big/\left[V_0^2(R_c^2 + X_c^2)(e^{2\alpha l} + e^{-2\alpha l} - 2\cos 2\theta)\right] \qquad (3)$$

$$Q_s / P_0 = \mathrm{Im}\left(\bar{V}_s \bar{I}_s^*\right)\big/P_0 = Z_0 X_c \left[(e^{2\alpha l} - e^{-2\alpha l})V_s^2 - 2V_s V_r e^{\alpha l}\cos(\theta+\delta) + 2V_s V_r e^{-\alpha l}\cos(\theta-\delta)\right]\big/\left[V_0^2(R_c^2 + X_c^2)(e^{2\alpha l} + e^{-2\alpha l} - 2\cos 2\theta)\right]$$
$$+ Z_0 R_c \left[2V_s^2 \sin 2\theta - 2V_s V_r e^{\alpha l}\sin(\theta+\delta) - 2V_s V_r e^{-\alpha l}\sin(\theta-\delta)\right]\big/\left[V_0^2(R_c^2 + X_c^2)(e^{2\alpha l} + e^{-2\alpha l} - 2\cos 2\theta)\right] \qquad (4)$$

As was described in [2-8], one practical way to increase power transfer level capability of a long line is to apply the technique of sectioning. For example, a shunt reactive power compensator could be installed at the midpoint of the line. As shown in Figure 3(a), each half of the line may then be represented by its π-equivalent circuit. The terminal synchronous equivalent sources G_1 and G_2 are ideal voltage sources and are assumed able to keep their respective terminal voltages constant. Suppose the midpoint (m) of the line is to be connected with a shunt reactive power compensator whose susceptance is B_γ, shown as the variable shunt in Figure 3(a). As defined in [8], the degree of compensation of the central half of the line at the midpoint is

$$k_m = B_\gamma / B_c \qquad (7)$$

k_m is arbitrarily taken as positive if B_γ is inductive and negative if B_γ is capacitive, B_c is the shunt susceptance of the whole line. In practical networks, however, the synchronous sources, the associated transformers and transmission systems connected to the line ends would have their respective impedances. The short-circuit impedances at the two ends should therefore be included in the analysis. In Figure 3(a), the values of these impedances are denoted as $R_{ti}+jX_{ti}$ at the respective line end where i = 1, 2. In this model, 1 denotes the SE whereas 2 denotes the RE. The authors of [5] have also included such impedances into their analysis.

(a)

(b)
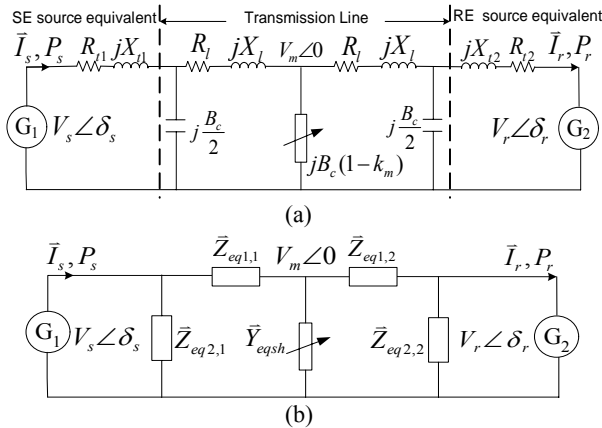
Figure 3: Equivalent circuit of a radial line with midpoint compensation and source impedances.

At fundamental frequency and through a series of Δ-Y transformations, the equivalent circuit shown in Figure 3(a) reduces to Figure 3(b). The equivalent impedance $\bar{Z}_{eq1,i}$, $\bar{Z}_{eq2,i}$ and $\bar{Y}_{eqsh}$ for the equivalent circuit shown in Figure 3(b) are given in Appendix B.

The above expressions show that once the line parameters and source equivalent impedances are known and the degree of compensation (k_m) is given, the equivalent network impedance and admittance values of Figure 3(b) can be determined.

Suppose the midpoint voltage is treated as the refer-ence phasor, i.e. $\bar{V}_m = V_m \angle 0^0$. Denote $\bar{V}_s = V_s \angle \delta_s$ and $\bar{V}_r = V_r \angle \delta_r$. Note that in this case, the power angle δ referred to in Section 2.1 is given as $\delta = \delta_s - \delta_r$.

From Figure 3(b), the following basic circuit equations are obtained:

$$(\bar{V}_s - \bar{V}_m)/\bar{Z}_{eq1,1} - (\bar{V}_m - \bar{V}_r)/\bar{Z}_{eq1,2} = \bar{Y}_{eqsh}\bar{V}_m \qquad (8)$$

$$\bar{I}_r = (\bar{V}_m - \bar{V}_r)/\bar{Z}_{eq1,2} - \bar{V}_r/\bar{Z}_{eq2,2} \qquad (9)$$

From (9), P_r can be derived:

$$P_r = \text{Re}(\bar{V}_r \bar{I}_r^*)$$
$$= V_r V_m (G_{eq1,2} \cos\delta_r + B_{eq1,2} \sin\delta_r) - V_r^2 (G_{eq1,2} + G_{eq2,2}) \quad (10)$$

The above expressions are too general and cannot be readily solved. However, P_r can be determined if the practical assumption is made that $V_s = V_r = V_0$. When normalized to P_0, P_r is given by

$$P_r/P_0 = Z_0(\alpha_{11}G_{eq1,2} - \alpha_{12}B_{eq1,2})\cos\delta - Z_0(\alpha_{11}B_{eq1,2} + \alpha_{12}G_{eq1,2})\sin\delta$$
$$+ Z_0(\alpha_{21}G_{eq1,2} - \alpha_{22}B_{eq1,2} - G_{eq1,2} - G_{eq2,2}) \qquad (11)$$

where the constant parameters α_{ij}, $G_{eqk,j}$, $B_{eqk,j}$ are given in Appendix C and can be readily determined.

With dynamic network control, the mid-point compensation susceptance is continuously regulated in such a way as to keep V_m constant such that $V_m = V_0$. Substitute $V_m = V_0$ into (8), one can show that the degree of compensation k_m is given by

$$k_m = 1 - (B_{eqsh} - B_{eq3,1} - B_{eq3,2})/B_c \qquad (12)$$

where

$$B_{eqsh} = G_{eq1,1}\sin\delta_s + B_{eq1,1}\cos\delta_s + G_{eq1,2}\sin\delta_r + B_{eq1,2}\cos\delta_r$$
$$- B_{eq1,1} - B_{eq1,2} \qquad (13)$$

Furthermore, recognizing that $\delta = \delta_s - \delta_r$ and since $V_m = V_s = V_r = V_0$, the derivation shown in Appendix D allows (14) and (15) (shown below) to be solved. The equations for the determination of δ_1, δ_2 and β_i are expressed in term of the known line parameters described in Figure 3(b). The detailed expressions are also given in Appendix D.

$$\delta_r = \delta_2 - \delta_1 \qquad (14)$$

Hence, for a given receiving-end power P_r, the following steps can be used to evaluate the shunt reactive compensation required at the midpoint of a transmission line in order to keep $V_m = V_s = V_r = V_0$:

Step 1: For a given P_r, use equation (15) to determine δ through numerical means as all the other parameters on the RHS of (15) are known.

Step 2: Determine δ_1 and δ_2 using the expressions (D.5) and (D.6) given in Appendix D.

Step 3: Use (14) to determine δ_r. δ_s can then be obtained since $\delta_s = \delta + \delta_r$.

Step 4: Equation (13) is used to solve for B_{eqsh} and use (12) to obtain k_m.

Step 5: From the definition of k_m in (7), reactive compensation B_γ needed at the mid-point is determined as $B_\gamma = k_m B_c$.

$$P_r/P_0 = Z_0 \left(\beta_4 G_{eq1,2} - B_{eq1,2}\sqrt{\beta_5 + \beta_2\cos\delta - \beta_3\sin\delta}\right)\left(G_{eq1,1}\cos\delta - B_{eq1,1}\sin\delta + G_{eq1,2}\right)\Big/\left(\beta_1 + \beta_2\cos\delta - \beta_3\sin\delta\right)$$

$$- Z_0 \left(\beta_4 B_{eq1,2} + G_{eq1,2}\sqrt{\beta_5 + \beta_2\cos\delta - \beta_3\sin\delta}\right)\left(G_{eq1,1}\sin\delta + B_{eq1,1}cos\delta + B_{eq1,2}\right)\Big/\left(\beta_1 + \beta_2\cos\delta - \beta_3\sin\delta\right) - Z_0\left(G_{eq1,2} + G_{eq2,2}\right) \qquad (15)$$

Equation (11) allows P_r/P_0 to be determined as a function of δ for a given k_m. A series of curves with varying amplitudes, each corresponds to a fixed value of B_γ, can be constructed. These curves are as shown in Figure 4. The controlling effect of the midpoint compensator constrains the operating point to move along the locus given by Equation (15), passing smoothly from one constant B_γ curve to another as P_r varies. With a practical compensator, of course, there is a limit to B_γ. When the limit is reached the compensator ceases to maintain constant voltage at its terminals and behaves instead like a fixed susceptance. The operating point then leaves the characteristic curve (15) and moves onto the constant B_γ curve under its maximum value $B_{\gamma max}$. The corresponding maximum power that can be transmitted represents the steady-state stability limit. This corresponds to the point A in Figure 4. If source resistances, line losses and capacitances have been excluded from (15), one can re-evaluate the P_r - δ curve. This is shown as curve (e) in Figure 4. From the figure, it can also be seen that with the same maximum level of compensation $B_{\gamma max}$, the $P_r - \delta$ curve derived using the simplified line model (curve (e)) is above that for the exact line model (curve (d)). Hence the predicted maximum power transfer level based on the lossless line assumption, such as that described in [3]-[8], would be slightly over-optimistic.
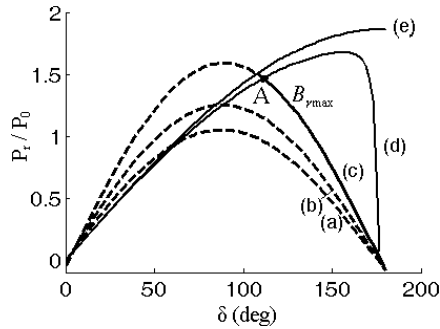
Figure 4: $P_r - \delta$ characteristics of a shunt-compensated line with $V_s = V_r = V_0$: (a) $B_\gamma = 0$; (b) $B_\gamma = 0.5/Z_0$; (c) $B_\gamma = B_{\gamma max}$; (d) exact line model with variable B_γ and $V_m = V_0$; (e) lossless line model with variable B_γ, $V_m = V_0$.

2.3 Maximum Power Transfer

In order to determine the steady-state stability limit of a midpoint compensated line, one can make use of (15) by differentiating P_r with respect to δ and set the resulting equation to zero. The resulting expression $f(\delta)$ is rather tedious and is shown in Appendix E. No analytical solution to it can be readily found unless some assumptions are made. Instead, it is proposed that through numerical means such as that based on the Bisection method [10], one solves for the angle δ by which the limit occurs. This angle is denoted as the critical angle, δ_{cr}. Essentially the numerical iterative procedure is used to find the roots of $f(\delta)=0$.

The maximum power that can be transferred is denoted herewith as P_{r1}^m. It can be obtained by replacing δ with δ_{cr} in (15). As described in Section 2.2, in practice there is an economic limit placed on the reactive power rating of the compensator. When the limit is reached the

compensator ceases to maintain constant voltage at its terminals and behaves like a fixed susceptance. The operating point then moves on to the constant B_γ curve corresponding to the maximum value of B_γ, i.e., $B_{\gamma max}$. The corresponding maximum power can be evaluated by reversing the numerical procedure described in Section 2.2. As shown in Figure 4, note that even without a limit on B_γ, maximum power does not occur at $\delta = 180°$ when line losses are included, unlike the case under the lossless line assumption described in [3-8].

3   NUMERICAL EXAMPLES

The following examples are based on the 500-kV transmission line used in [11] where $R = 0.01755$ Ω/km, $L = 0.0008737$ H/km, $C = 0.01333$ uF/km and $G = 0$. For convenience, it is also assumed that the terminal impedances are identical, i.e. $\bar{Z}_{t1} = \bar{Z}_{t2} = Z_t \angle \theta_t$.

3.1 Effect of Terminal Impedances on Power Transfer

The total impedances appearing at the end(s) of the line add to the series transfer impedances and alter the phase angle difference between the SE and RE voltages. The effect of the impedances is therefore to increase δ for a given P_r, as illustrated in Figure 5(a). Figure 5(b) shows the ratio of the maximum power transfer with mid-point compensation (P_{r1}^m) to that without midpoint compensation (P_{r0}^m). This ratio is plotted against Z_t under varied line length. It can be seen that Z_t will reduce the benefit obtainable from the midpoint compensator. The reduction increases more significantly with the increase in line length. For example, Figure 5(b) shows that with the common practice of mid-point shunt compensation at a regular 350-km (200-miles) interval, a 700-km line would see its maximum power level at about 1.6 times that without compensator and if $Z_t = 0.11 Z_0$.

| (a) | (b) |
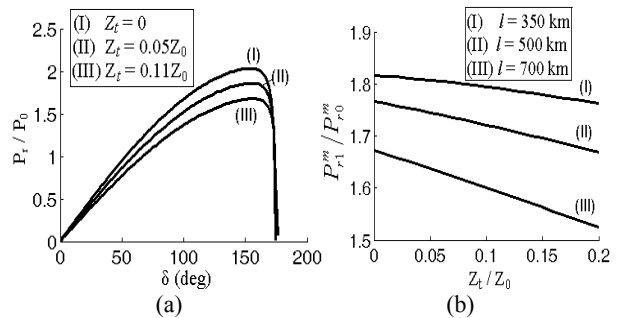
Figure 5: Effect of line terminal impedances on (a) the $P_r - \delta$ characteristic and (b) the steady-state stability limit of a midpoint compensated line.

3.2 Effect of Line Losses on Steady-state Stability Limit

Figure 6 shows the P_r- δ characteristic of the 700-km line when it is assumed that $Z_t = 0.11Z_0$ and has an impedance angle of 89^0 [11]. From Figure 6(a), it can be seen that as the line becomes more resistive, P_{rmax1} reduces. For the same level of power transmission, δ tends to increase as R_l / X_l increases. Furthermore, the line resistance will reduce the benefit that can be derived from the midpoint compensator. The larger the R_l / X_l ratio, the larger reduction in the benefit of the mid-point

compensation is observed. This is indicated clearly in Figure 6(b).
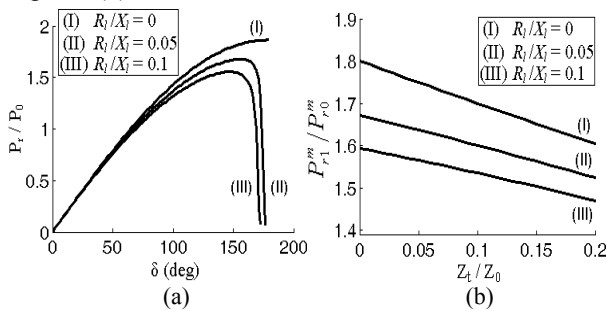
Figure 6: Effect of line resistances on (a) the δ-P_r characteristic and (b) reducing the benefit under dynamic midpoint compensation

3.3 General Observation on the Benefit of Midpoint Compensation

Steady-state transfer capability of long transmission lines and the extent such capability can be enhanced through midpoint shunt compensation can now be elaborated on. Table 1 summarizes the maximum power transfer calculated using the expressions contained in Section II for the same 700-km, 500-kV line and terminal conditions as given in Section 3.2. Assume that the compensator is able to maintain the midpoint voltage at V_0 with ideal instantaneous response. Four line models have been considered. Using the simplified line model in which only the line series reactance has been included, it has been shown earlier that with mid-point compensation, the maximum power that can be transmitted with respect to the steady-state stability limit is increased by a factor of 2. This can be seen by examining the results of Case 1 in Table 1. However this factor is an overly optimistic assessment in predicting the beneficial effect of the shunt compensator. When line losses are included (Case 2), this factor reduces to 1.87. In Case 3 in which the equivalent π-circuit model with no losses shows that the steady-state stability limit is $2.2976P_0$ as against $2.2208P_0$ shown in Case 1. The difference is due to the presence of the line capacitance: the capacitance provides additional support on the power transfer, an effect the simplified line model does not take into consideration. Hence the simplified line model over-estimates the beneficial effect of mid-point compensator on improving steady-state stability limit. With the line losses included in the model, it predicts a further decrease of the limit by some 13%. This can be seen by comparing the results of Cases 3 and 4.

The most accurate line model amongst the four would be the one based on the Telegraph equations. When the terminal impedance is included in the example, a further reduction of the limit is obtained, as shown in Cases 5-8. Case 8 shows that the beneficial effect of the mid-point compensation is about 1.59 times that without the compensation. This agrees fairly closely with that obtained in [5]. Unlike the observations shown in [5] which were based on computer simulation, the predicted values shown in Table 1 were obtained using the analytical expressions derived in Section 2.2. Hence the

analytical expressions shown are most useful: they provide the theoretical basis in quantifying the various factors that could affect the steady-state stability limit of a compensated line.

Case		P_{r0}^m / P_0	P_{r1}^m / P_0	P_{r1}^m / P_{r0}^m
Without terminal impedances	1: Simplified loss-less line model	1.1104	2.2208	2
	2: Simplified line model with losses	1.0498	1.9582	1.87
	3: Telegraph loss-less line model	1.2760	2.2976	1.80
	4: Telegraph line model with losses	1.2161	2.0338	1.67
With terminal impedances	5: Simplified lossless line model	0.8884	1.7768	2
	6: Simplified line model with losses	0.8465	1.5911	1.88
	7: Telegraph loss-less line model	1.0947	1.8637	1.70
	8: Telegraph line model with losses	1.0522	1.6774	1.59

Table 1: Effect of line model representation on steady-state stability limits.

In order to verify the accuracy of the earlier analysis, time-response simulation studies have to be carried out. Further work will be needed in extending the above results for more complex networks.

4 CONCLUSIONS

Shunt compensation of a long-line at terminals and at mid-point has been considered. By utilizing the exact long-line model which includes line losses, the results of the analysis allow the effect of line resistance on the amount of the reactive compensation needed for power transfer to be determined much more accurately. Impedances of the line terminal synchronous sources have been included in the determination.

An important application of the results of the analysis is that the reactive power needed at the line midpoint at any given power transfer level can be determined using the computational procedure described. Re-evaluation of the contribution of the midpoint shunt compensator to enhance stability shows that whereas in previous works based on simplified line model, the improvement in power transmissibility with respect to the steady-state stability limit is predicted to increase by a factor of 2, the present analysis indicates that the improvement is only by a factor of 1.67. The decrement is accounted for due to the presence of line resistances and the distributed nature of the line shunt capacitances. If the terminal impedances at the end(s) of the line are also included, there is a further reduction in the factor to around 1.59.

The analysis provides a more accurate assessment of the beneficial contribution of shunt reactive power compensation. Additional insights into the steady-state transfer capability of long transmission lines have therefore been gained.

REFERENCES

[1] B.F. Wollenberg, "Transmission system reactive power compensation", PES Winter Meeting, 2002. IEEE, Vol.1, 27-31 Jan. 2002, pp. 507 - 508

[2] E. W. Kimbark, "A new look at shunt compensation", IEEE Trans on Power App. Syst., Vol. PAS-102, No.1, pp. 212-218, Jan 1983.

[3] E.W. Kimbark, "How to improve system stability without risking sub-synchronous resonance," IEEE Trans. Power App. Syst., Vol. PAS-96, No. 5, pp. 1608-1619, Sep./Oct. 1977.

[4] B.T. Ooi, M. Kazerani, Z. Wolanski, F.D. Galiana and G. Joos, "Midpoint siting of FACTS devices in transmission lines," IEEE Trans. Power Delivery, Vol.12, No.4, pp.1717-1722, Oct. 1997.

[5] Z. Huang; B.T. Ooi, "Power transfer capability of long transmission lines with midpoint sited FACTS and HVDC", Power Engineering Review, IEEE, Vol.22, No. 5, pp. 51-53, May 2002.

[6] P. Kundur, "Power System stability and control". New York: McGraw Hill, 1994.

[7] C.W. Taylor, "Power System Voltage Stability". New York: McGraw Hill, 1994.

[8] T. J. E. Miller, Reactive Power Control in Electric Systems. New York: Wiley, 1982.

[9] E.M. Anderson, "Electric Transmission Line Fundamentals". Reston Publishing Company, 1985.

[10] S.S. Rao, "Applied Numerical Methods for Engineers and Scientists", Prentice Hall, 2002.

[11] G. Sybille, P. Giroux, "Simulation of FACTS controllers using the MATLAB Power System Blockset and Hypersim real-time simulator", PES Winter Meeting, IEEE, Vol. 1, pp. 488 – 491, Jan. 2002.

Appendix A
Derivation of Equations (1)- (4)

From [6], assume that voltage $\vec{V}_r$ and current $\vec{I}_r$ are known at the RE ($x = 0$), thus the general expressions for voltage and current at a distance x from the RE are

$$\vec{V}_x = \left[\left(\vec{V}_r + \vec{Z}_c \vec{I}_r \right) e^{\vec{\gamma} x} + \left(\vec{V}_r - \vec{Z}_c \vec{I}_r \right) e^{-\vec{\gamma} x} \right] / 2 \qquad (A.1)$$

$$\vec{I}_x = \left[\left(\vec{V}_r / \vec{Z}_c + \vec{I}_r \right) e^{\vec{\gamma} x} - \left(\vec{V}_r / \vec{Z}_c - \vec{I}_r \right) e^{-\vec{\gamma} x} \right] / 2 \qquad (A.2)$$

From (A.1), with $x = l$, (A.3) can be obtained.

$$\vec{V}_s = \left[\left(\vec{V}_r + \vec{Z}_c \vec{I}_r \right) e^{\vec{\gamma} l} + \left(\vec{V}_r - \vec{Z}_c \vec{I}_r \right) e^{-\vec{\gamma} l} \right] / 2 \qquad (A.3)$$

Hence, the current at the RE of a transmission line can be written as:

$$\vec{I}_r = \left[2\vec{V}_s - \vec{V}_r (e^{\gamma l} + e^{-\gamma l}) \right] / \left[\vec{Z}_c (e^{\gamma l} - e^{-\gamma l}) \right] \qquad (A.4)$$

From Equations (A.2) and (A.4), with $x = l$, (A.5) can be obtained.

$$\vec{I}_s = \left[\vec{V}_s (e^{\vec{\gamma} l} + e^{-\vec{\gamma} l}) - 2\vec{V}_r \right] / \left[\vec{Z}_c (e^{\vec{\gamma} l} - e^{-\vec{\gamma} l}) \right] \qquad (A.5)$$

Since $\theta = \beta l$, equations (A.4) and (A.5) can be rewritten as (A.6) and (A.7), respectively:

$$\vec{I}_r = \frac{2\vec{V}_s - \vec{V}_r[e^{\alpha l}(\cos\theta + j\sin\theta) + e^{-\alpha l}(\cos\theta - j\sin\theta)]}{(R_c + jX_c)[e^{\alpha l}(\cos\theta + j\sin\theta) - e^{-\alpha l}(\cos\theta - j\sin\theta)]} \quad (A.6)$$

$$\vec{I}_s = \frac{\vec{V}_s[e^{\alpha l}(\cos\theta + j\sin\theta) + e^{-\alpha l}(\cos\theta - j\sin\theta)] - 2\vec{V}_r}{(R_c + jX_c)[e^{\alpha l}(\cos\theta + j\sin\theta) - e^{-\alpha l}(\cos\theta - j\sin\theta)]} \quad (A.7)$$

It can be derived that the active and reactive powers at the RE and SE of a transmission line are given by Equations (A.8) and (A.9) (shown below), respectively. The normalized values with respect to P_0 of P_r, Q_r, P_s and Q_s can be obtained as shown in Equations (1) –(4).

Appendix B
Expressions for the Equivalent Impedances and Admittance of Figure 3 (b)

$\vec{Z}_{eq1,i} = R_{ti} + jX_{ti} + R_l + jX_l + jB_c(R_{ti} + jX_{ti})(R_l + jX_l)/2$;

$\vec{Z}_{eq2,i} = R_{ti} + jX_{ti} - j2/B_c - j2(R_{ti} + jX_{ti})/[B_c(R_l + jX_l)]$;

$\vec{Y}_{eqsh} = 1/\vec{Z}_{eqm,1} + 1/\vec{Z}_{eqm,2} + jB_c(1 - k_m)$;

$\vec{Z}_{eqm,i} = R_l + jX_l - j2/B_c - j2(R_l + jX_l)/[B_c(R_{ti} + jX_{ti})]$.

$$
\begin{aligned}
\vec{S}_r = P_r + jQ_r = \vec{V}_r \vec{I}_r^* &= \frac{2V_s V_r(\cos\delta - j\sin\delta) - V_r^2\left[e^{\alpha l}(\cos\theta - j\sin\theta) + e^{-\alpha l}(\cos\theta + j\sin\theta)\right]}{(R_c - jX_c)\left[e^{\alpha l}(\cos\theta - j\sin\theta) - e^{-\alpha l}(\cos\theta + j\sin\theta)\right]} \\[2mm]
&= \frac{R_c\left[2V_s V_r e^{\alpha l}\cos(\theta - \delta) - 2V_s V_r e^{-\alpha l}\cos(\theta + \delta) + V_r^2(e^{-2\alpha l} - e^{2\alpha l})\right] - X_c\left[2V_s V_r e^{\alpha l}\sin(\theta - \delta) + 2V_s V_r e^{-\alpha l}\sin(\theta + \delta) - 2V_r^2\sin 2\theta\right]}{(R_c^2 + X_c^2)(e^{2\alpha l} + e^{-2\alpha l} - 2\cos 2\theta)} \\[2mm]
&+ j\left\{\frac{X_c\left[2V_s V_r e^{\alpha l}\cos(\theta - \delta) - 2V_s V_r e^{-\alpha l}\cos(\theta + \delta) + V_r^2(e^{-2\alpha l} - e^{2\alpha l})\right] + R_c\left[2V_s V_r e^{\alpha l}\sin(\theta - \delta) + 2V_s V_r e^{-\alpha l}\sin(\theta + \delta) - 2V_r^2\sin 2\theta\right]}{(R_c^2 + X_c^2)(e^{2\alpha l} + e^{-2\alpha l} - 2\cos 2\theta)}\right\}
\end{aligned}
$$
$$(A.8)$$

$$
\begin{aligned}
\vec{S}_s = P_s + jQ_s = \vec{V}_s \vec{I}_s^* &= \frac{V_s^2\left[e^{\alpha l}(\cos\theta - j\sin\theta) + e^{-\alpha l}(\cos\theta + j\sin\theta)\right] - 2V_s V_r(\cos\delta + j\sin\delta)}{(R_c - jX_c)\left[e^{\alpha l}(\cos\theta - j\sin\theta) - e^{-\alpha l}(\cos\theta + j\sin\theta)\right]} \\[2mm]
&= \frac{R_c\left[(e^{2\alpha l} - e^{-2\alpha l})V_s^2 - 2V_s V_r e^{\alpha l}\cos(\theta + \delta) + 2V_s V_r e^{-\alpha l}\cos(\theta - \delta)\right] - X_c\left[2V_s^2\sin 2\theta - 2V_s V_r e^{\alpha l}\sin(\theta + \delta) - 2V_s V_r e^{-\alpha l}\sin(\theta - \delta)\right]}{(R_c^2 + X_c^2)(e^{2\alpha l} + e^{-2\alpha l} - 2\cos 2\theta)} \\[2mm]
&+ j\left\{\frac{X_c\left[(e^{2\alpha l} - e^{-2\alpha l})V_s^2 - 2V_s V_r e^{\alpha l}\cos(\theta + \delta) + 2V_s V_r e^{-\alpha l}\cos(\theta - \delta)\right] + R_c\left[2V_s^2\sin 2\theta - 2V_s V_r e^{\alpha l}\sin(\theta + \delta) - 2V_s V_r e^{-\alpha l}\sin(\theta - \delta)\right]}{(R_c^2 + X_c^2)(e^{2\alpha l} + e^{-2\alpha l} - 2\cos 2\theta)}\right\}
\end{aligned}
$$
$$(A.9)$$

Appendix C
Determination of P_r for line with fixed midpoint shunt compensator

Equation (8) can be rewritten as,

$$\vec{V}_m = V_s\left(\alpha_{11}\cos\delta_s - \alpha_{12}\sin\delta_s\right) + V_r\left(\alpha_{21}\cos\delta_r - \alpha_{22}\sin\delta_r\right)$$
$$+ j\left[V_s\left(\alpha_{11}\sin\delta_s + \alpha_{12}\cos\delta_s\right) + V_r\left(\alpha_{21}\sin\delta_r + \alpha_{22}\cos\delta_r\right)\right] \quad (C.1)$$

where $\alpha_{11} = \mathrm{Re}\left[\vec{Z}_{eq1,2}\Big/\left(\vec{Y}_{eqsh}\vec{Z}_{eq1,1}\vec{Z}_{eq1,2} + \vec{Z}_{eq1,2} + \vec{Z}_{eq1,1}\right)\right]$;

$\alpha_{12} = \mathrm{Im}\left[\vec{Z}_{eq1,2}\Big/\left(\vec{Y}_{eqsh}\vec{Z}_{eq1,1}\vec{Z}_{eq1,2} + \vec{Z}_{eq1,2} + \vec{Z}_{eq1,1}\right)\right]$;

$\alpha_{21} = \mathrm{Re}\left[\vec{Z}_{eq1,1}\Big/\left(\vec{Y}_{eqsh}\vec{Z}_{eq1,1}\vec{Z}_{eq1,2} + \vec{Z}_{eq1,2} + \vec{Z}_{eq1,1}\right)\right]$;

$\alpha_{22} = \mathrm{Im}\left[\vec{Z}_{eq1,1}\Big/\left(\vec{Y}_{eqsh}\vec{Z}_{eq1,1}\vec{Z}_{eq1,2} + \vec{Z}_{eq1,2} + \vec{Z}_{eq1,1}\right)\right]$.

Equating the real and imaginary parts of (C.1),

$$V_m = V_s\left(\alpha_{11}\cos\delta_s - \alpha_{12}\sin\delta_s\right) + V_r\left(\alpha_{21}\cos\delta_r - \alpha_{22}\sin\delta_r\right) \quad (C.2)$$

$$V_s\left(\alpha_{11}\sin\delta_s + \alpha_{12}\cos\delta_s\right) + V_r\left(\alpha_{21}\sin\delta_r + \alpha_{22}\cos\delta_r\right) = 0 \quad (C.3)$$

Since $\delta = \delta_s - \delta_r$, (C.2) $\cos\delta_r$ + (C.3) $\sin\delta_r$ becomes

$$V_m\cos\delta_r = \alpha_{11}V_s\cos\delta - \alpha_{12}V_s\sin\delta + \alpha_{21}V_r \quad (C.4)$$

Also (C.2) $\sin\delta_r$ - (C.3) $\cos\delta_r$ becomes

$$V_m\sin\delta_r = -\alpha_{11}V_s\sin\delta - \alpha_{12}V_s\cos\delta - \alpha_{22}V_r \quad (C.5)$$

From Figure 3(b),

$$\vec{I}_r = \left(\vec{V}_m - \vec{V}_r\right)\Big/\vec{Z}_{eq1,2} - \vec{V}_r\Big/\vec{Z}_{eq2,2} \quad (C.6)$$

Hence, for a given k_m, power at the receiving end is given by

$$P_r = \mathrm{Re}\left(\vec{V}_r\vec{I}_r^*\right)$$
$$= V_r V_m\left(G_{eq1,2}\cos\delta_r + B_{eq1,2}\sin\delta_r\right) - V_r^2\left(G_{eq1,2} + G_{eq2,2}\right) \quad (C.7)$$

where $G_{eqk,i} = \mathrm{Re}\left(1\big/\vec{Z}_{eqk,i}\right)$; $B_{eqk,i} = \mathrm{Im}\left(1\big/\vec{Z}_{eqk,i}\right)$.

Substitute (C.4) and (C.5) into (C.7), and if $V_s = V_r = V_0$, the value of P_r normalized to P_0 is

$$P_r/P_0 = Z_0\left(\alpha_{11}G_{eq1,2} - \alpha_{12}B_{eq1,2}\right)\cos\delta - Z_0\left(\alpha_{11}B_{eq1,2} + \alpha_{12}G_{eq1,2}\right)\sin\delta$$
$$+ Z_0\left(\alpha_{21}G_{eq1,2} - \alpha_{22}B_{eq1,2} - G_{eq1,2} - G_{eq2,2}\right) \quad (C.8)$$

Appendix D
Determination of P_r of loss line with dynamic network control

Equation (8) can be rewritten as,

$$\left[\left(G_{eq1,1} + G_{eq1,2} + G_{eqsh}\right) + j\left(B_{eq1,1} + B_{eq1,2} + B_{eqsh}\right)\right]\vec{V}_m$$
$$= \left(G_{eq1,1} + jB_{eq1,1}\right)\vec{V}_s + \left(G_{eq1,2} + jB_{eq1,2}\right)\vec{V}_r \quad (D.1)$$

where

$$G_{eqsh} = \mathrm{Re}\left(\vec{Y}_{eqsh}\right) = G_{eqm,1} + G_{eqm,2}\;;$$
$$B_{eqsh} = \mathrm{Im}\left(\vec{Y}_{eqsh}\right) = B_{eqm,1} + B_{eqm,2} + B_c(1 - k_m)\;.$$

Separating the real and imaginary parts of (D.1) leads to the following identities:

$$\left(G_{eq1,1} + G_{eq1,2} + G_{eqsh}\right)V_m = \left(G_{eq1,1}\cos\delta_s - B_{eq1,1}\sin\delta_s\right)V_s$$
$$+ \left(G_{eq1,2}\cos\delta_r - B_{eq1,2}\sin\delta_r\right)V_r \quad (D.2)$$

$$\left(B_{eq1,1} + B_{eq1,2} + B_{eqsh}\right)V_m = \left(G_{eq1,1}\sin\delta_s + B_{eq1,1}\cos\delta_s\right)V_s$$
$$+ \left(G_{eq1,2}\sin\delta_r + B_{eq1,2}\cos\delta_r\right)V_r \quad (D.3)$$

Equation (D.2) can be rewritten as:

$$G_{eq1,1} + G_{eq1,2} + G_{eqsh} = \left(G_{eq1,1}\cos\delta - B_{eq1,1}\sin\delta + G_{eq1,2}\right)\cos\delta_r$$
$$- \left(G_{eq1,1}\sin\delta + B_{eq1,1}\cos\delta + B_{eq1,2}\right)\sin\delta_r \quad (D.4)$$

Define the following two intermediate variables

$$\delta_1 = -\cos^{-1}\left[\frac{\left(G_{eq1,1}\cos\delta - B_{eq1,1}\sin\delta + G_{eq1,2}\right)}{\sqrt{\left(G_{eq1,1}\cos\delta - B_{eq1,1}\sin\delta + G_{eq1,2}\right)^2 + \left(G_{eq1,1}\sin\delta + B_{eq1,1}\cos\delta + B_{eq1,2}\right)^2}}\right]$$
$$(D.5)$$

$$\delta_2 = -\cos^{-1}\left[\frac{\left(G_{eq1,1} + G_{eq1,2} + G_{eqsh}\right)}{\sqrt{\left(G_{eq1,1}\cos\delta - B_{eq1,1}\sin\delta + G_{eq1,2}\right)^2 + \left(G_{eq1,1}\sin\delta + B_{eq1,1}\cos\delta + B_{eq1,2}\right)^2}}\right]$$
$$(D.6)$$

Substitute (D.5) and (D.6) into (D.4) and express the resulting equation in term of δ_1, δ_2 and δ_r. Then the following equation can be obtained:

$$\cos\delta_2 = \cos\delta_r\cos\delta_1 - \sin\delta_r\sin\delta_1 \quad (D.7)$$

Substitute Equations (D.5), (D.6) and (D.7) into (10), (15) can be obtained. Where,

$\beta_1 = G_{eq1,1}^2 + G_{eq1,2}^2 + B_{eq1,1}^2 + B_{eq1,2}^2$; $\beta_2 = 2\left(G_{eq1,1}G_{eq1,2} + B_{eq1,1}B_{eq1,2}\right)$;

$\beta_3 = 2\left(B_{eq1,1}G_{eq1,2} - G_{eq1,1}B_{eq1,2}\right)$; $\beta_4 = G_{eq1,1} + G_{eq1,2} + G_{eqsh}$;

$\beta_5 = B_{eq1,1}^2 + B_{eq1,2}^2 - G_{eqsh}^2 - 2G_{eq1,1}G_{eq1,2} - 2G_{eq1,1}G_{eqsh} - 2G_{eq1,2}G_{eqsh}$.

Appendix E
Determination of critical angle δ_{cr} of a midpoint compensated line with dynamic network control

From (15), the following expression (E.1) can be obtained:

$$f(\delta) = \frac{dP_r}{d\delta} = \frac{V_0^2\left(G_{eq1,1}G_{eq1,2} - B_{eq1,1}B_{eq1,2}\right)\left(\beta_3\beta_4 - \beta_2\sqrt{\beta_5 + \beta_2\cos\delta - \beta_3\sin\delta} - \beta_1\sqrt{\beta_5 + \beta_2\cos\delta - \beta_3\sin\delta}\cos\delta - \beta_1\beta_4\sin\delta\right)}{\left(\beta_1 + \beta_2\cos\delta - \beta_3\sin\delta\right)^2}$$

$$+ \frac{V_0^2\left(\beta_2\sin\delta + \beta_3\cos\delta\right)\left[\beta_4\left(G_{eq1,2}^2 - B_{eq1,2}^2\right) - 2G_{eq1,2}B_{eq1,2}\sqrt{\beta_5 + \beta_2\cos\delta - \beta_3\sin\delta}\right]}{\left(\beta_1 + \beta_2\cos\delta - \beta_3\sin\delta\right)^2}$$

$$- \frac{V_0^2\left(G_{eq1,1}B_{eq1,2} + G_{eq1,2}B_{eq1,1}\right)\left(\beta_2\beta_4 + \beta_3\sqrt{\beta_5 + \beta_2\cos\delta - \beta_3\sin\delta} + \beta_1\beta_4\cos\delta - \beta_1\sqrt{\beta_5 + \beta_2\cos\delta - \beta_3\sin\delta}\sin\delta\right)}{\left(\beta_1 + \beta_2\cos\delta - \beta_3\sin\delta\right)^2}$$

$$+ \frac{V_0^2\left(\beta_2\sin\delta + \beta_3\cos\delta\right)\left[\left(G_{eq1,1}G_{eq1,2} - B_{eq1,1}B_{eq1,2}\right)\sin\delta + \left(G_{eq1,2}B_{eq1,1} + G_{eq1,1}B_{eq1,2}\right)\cos\delta + 2G_{eq1,2}B_{eq1,2}\right]}{2\left(\beta_1 + \beta_2\cos\delta - \beta_3\sin\delta\right)\sqrt{\beta_5 + \beta_2\cos\delta - \beta_3\sin\delta}} \quad (E.1)$$